The Experiment and Analysis of Image Acquisition System Based on the Hardware Platform

Baoju Zhang, Lei Xue, Shan Qin, Dan Wang and Yulong Gu

Abstract This paper introduced the hardware platform of image measurement reconstruction which is based on the theory of the compression sensing and its working process, the hardware platform consists of two parts, front-end acquisition circuit and rear reconstruction port. Acquisition port uses the Complementary Metal Oxide Semiconductor(CMOS) image sensor, it can achieve the real-time image acquisition, deposit the image in memory which is acquired in real time through a peripheral interface, to generate the corresponding gray level matrix. Then completing the transplantation of image reconstruction algorithm and the debugging of program through the hardware platform of the image measurement and the reconstruction system, achieving the reconstruction of Chinese characters and the complex image quiet clearly.

Keywords Compressive sensing · Image acquisition · Image reconstruction

1 Introduction of Image Acquisition System

The hardware platform of image acquisition system is shown in Fig. 1, it includes power supply unit, complementary metal oxide semiconductor (CMOS) image sensor [1], storage unit, central processing unit, image display screen, and communication unit, and its overall structure is shown in Fig. 1. The working voltage of power supply unit for other units to provide appropriate. The working process of image acquisition system is as follows:

(1) CMOS image sensor, which is in the front-end of the system [2], is responsible for the image acquisition in real time, the generated RGB image matrix visiting the access controller DMA through direct memory of the processor in

B. Zhang (✉) · L. Xue · S. Qin · D. Wang · Y. Gu
College of Electronic and Communication Engineering,
Tianjin Normal University, Tianjin, China
e-mail: wdxyzbj@163.com

Q. Liang et al. (eds.), *Proceedings of the 2015 International Conference on Communications, Signal Processing, and Systems*, Lecture Notes in Electrical Engineering 386, DOI 10.1007/978-3-662-49831-6_90

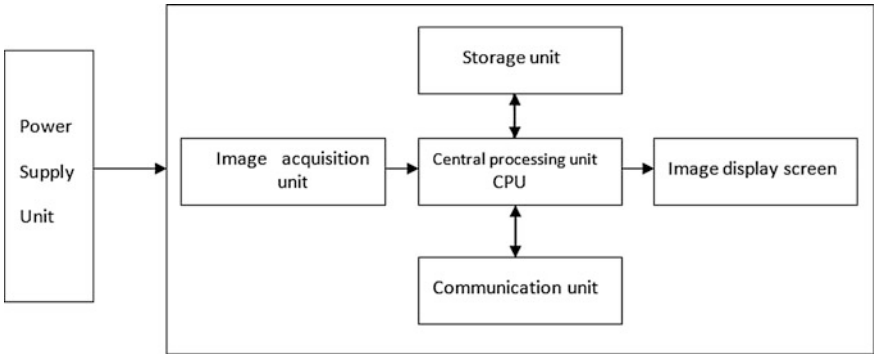

Fig. 1 Structure chart of image acquisition system

central processing unit [3], can be stored in the storage unit directly, have no need to occupy the resource of central processor unit CPU;

(2) The RGB image, which is stored in the storage unit, make it a gray one by processor to generate a corresponding two-dimensional matrix of the gray image, and then observing and reconstructing the two-dimensional matrix of the gray image by reconstructing image observation program;

(3) Finally, displaying the reconstructed gray-scale image through the image display screen;

(4) The whole working process is controlled by the upper machine through the communication module.

1.1 The Introduced of Processor OMAPL138

The embedded application processor with Da Vinci architecture of TI company started to use the combination of DSP [4] and ARM, which has the asymmetric nuclear structure [5], OMAPL138, as a classic processor, is a dual-core processor with low consumption. Dual-core architecture in OMAPL138, combined the advantages of high-speed digital signal processing performance in DSP and Reduced Instruction Set Computer (RISC) [6] in ARM, used TMS320C674xDSP kernel and ARM926EJ-S kernel which both have high performance. The internal resources structure of OMAPL138 is shown in Fig. 2.

2 Image Signal Measurement and Display Unit

Image signal acquisition unit, which used OV2640 image sensor, connected the processor OMAPL138 through the VPIF interface.

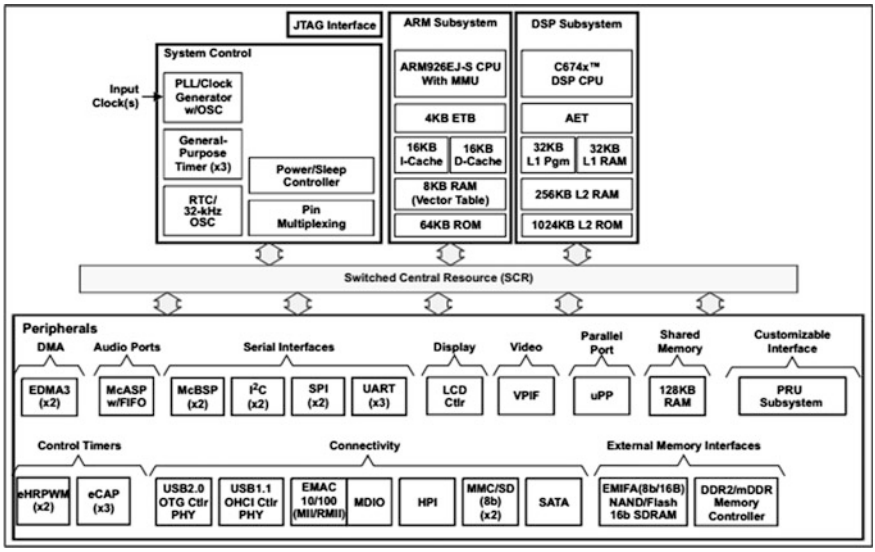

Fig. 2 The resource structure of OMAPL138

2.1 The Profile of Image Sensor OV2640

OV2640 is a CMOS image sensor [7], the first video sensor with 0.25 inches size and 2-million pixels, is a new image sensor with the architecture of 2.2 micron OmniPixel2. It can be assembled into mm-scale socket products, which is currently one of the miniature camera module. OV2640 uses high-tech and advanced OmniPixel2 architecture, with a richer color and zero-gap micro-lens structure, to increase the fill factor and quantum, and form a sensitive 2.2 micron pixel, improving the efficiency and effect of display [8]. Besides the benefits that OmniPixel2 architecture has brought, OmniVision integrates the advanced image signal processing module (OmniQSP), greatly improving the performance of the image. OV2640 has five units, including the analog signal processing unit, 10-bit A/D converter, digital signal processing unit, output format specification unit, and compression unit, it also has microcontroller, SCCB peripheral interface, and digital video output interface, Fig. 3 shows its internal structure function. It has the following features:

(1) Supporting 2-million pixels;
(2) Resolution can be as high as 1632 × 1232, as well supporting 320 × 240, 640 × 480, 800 × 600, 1024 × 768 [9];
(3) The refresh rate can be 30 frames/s, the rate is accessible in the highest yield 60 frames/s.

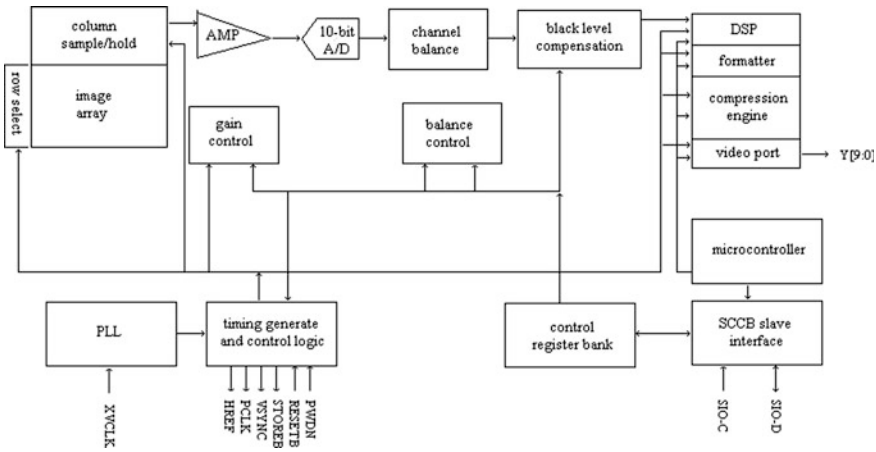

Fig. 3 The internal functional structure of image sensor OV2640

2.2 *Image/Video Peripheral Interface VPIF*

Image sensor OV2640 is connected to the processor OMAPL138 through VPIF interface, VPIF interface can capture and display the digital video. OMAPL138 VPIF interface includes two video input channels and two video output channels. Input channel 0 and input channel 1 share the same receiving structure, and output channel 2 and output channel 3 share the same transmission structure. Input and output channels of VPIF are as shown in Fig. 4. It has two input and output channels with embedded time code for 8-bit standard definition video signal, one input and output channel with embedded time code for 16-bit high definition video signals, and one input channel for 16-bit original video signal.

VPIF interface has four clock input pins and 2 clock output pins. Each channel has one clock input pin [10], can achieve the control of clock edges through the

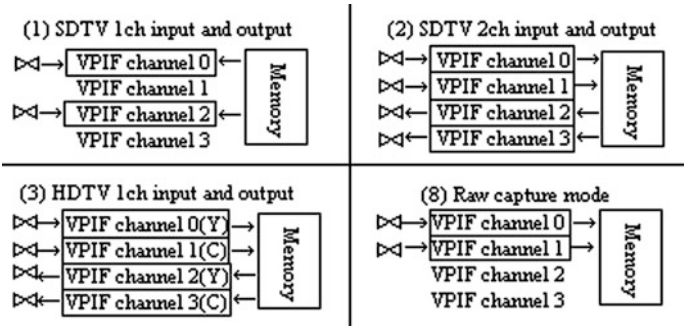

Fig. 4 The figure of input and output channels of VPIF

CLKEDGE which is in the register CnCTRL, 1, 2, 3 (n = 0), which is corresponding to each channel. VPIF interface can provide clocks for external devices through channels 2 and 3, and accomplish the setting of devices through the CLKEN digit in C2CTRL and C3CTRL registers which is corresponding to channels 2 and 3. The clock frequency produced by VPIF interface has the same frequency with input clock signal.

In this system, the image sensor OV2640 connect with OMAPL138 through VPIF interface, configuring VPIF interface as raw capture mode, in this mode, the output signal of image sensor can be transmitted to the processor directly. Processor can access controller DMA through direct memory to deposit data in the storage unit directly, do not take up the resource of CPU. In general, the format of the output signal which is produced by image sensor is RGB (sometimes can be RGrGbB). The format of the signal has the following characteristics:

(1) Storing the pixel data directly;
(2) Data bit width can be 8-bit pixels, 10-bit pixels or 12-bit pixels;
(3) Having selections of horizontal and vertical pixel signal polarity;
(4) Storing fields separately and crosswise.

2.3 LCD Display Unit

The image display unit adopts the AT070TN83 display screen made by INNOLUX Corporation. AT070TN83 is a 7-inch TFT-LCD screen, whose color-depth format is 16-bit RGB565, resolution with 800 × 400 pixel units, satisfies the need of displaying. AT070TN83 connects with the processor OMAPL138 through VPIF interface.

3 Experiments on the Hardware Platform

There are two sets of experiment in this paper. Experiment 1 used GPSR reconstruction algorithm combining with polynomial measurement matrix based on gram matrix. Experiment 2 used SAMP algorithm combining with Hada code measurement matrix based on pseudo-random sequence.

3.1 Experiment 1: GPSR Reconstruction Algorithm Combining with Polynomial Measurement Matrix Based on Gram Matrix

The GPSR algorithm adopted in the experiment combining with polynomial matrix measurement which based on gram matrix, the experiment was divided into three

groups. Each test adopted different measurement ratios, respectively, 20 %, 30 %, and 40 %. Two of these tests were simple Chinese character' images, "天" and "津"; the third group test is for the typical and quietly complex Lena image.

3.1.1 The Experimental Data

Figure 5 shows the corresponding reconstruction rendering of word "天" under different measurement ratios, Fig. 6 shows the corresponding reconstruction effect of word "津" under different measurement ratios, and Fig. 7 shows the corresponding reconstruction effect of the Lena image under the different measurements ratios. Table 1 shows the reconstruction time in each group under the different measurement ratios.

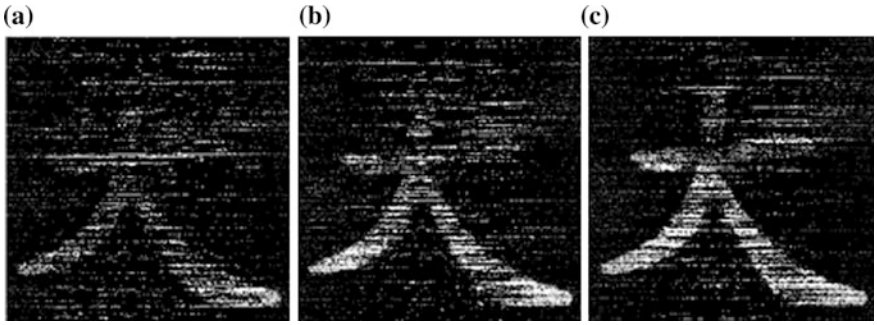

Fig. 5 The reconstruction effect chart of word "天". **a** Ratio is 20 %. **b** Ratio is 30 %. **c** Ratio is 40 %

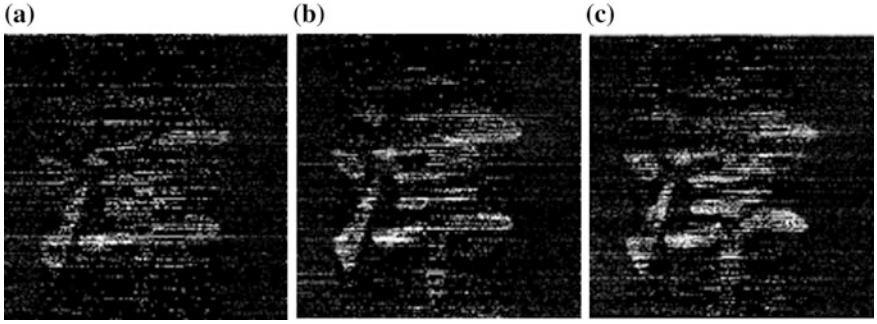

Fig. 6 The reconstruction effect chart of word "津". **a** Ratio is 20 %. **b** Ratio is 30 %. **c** Ratio is 40 %

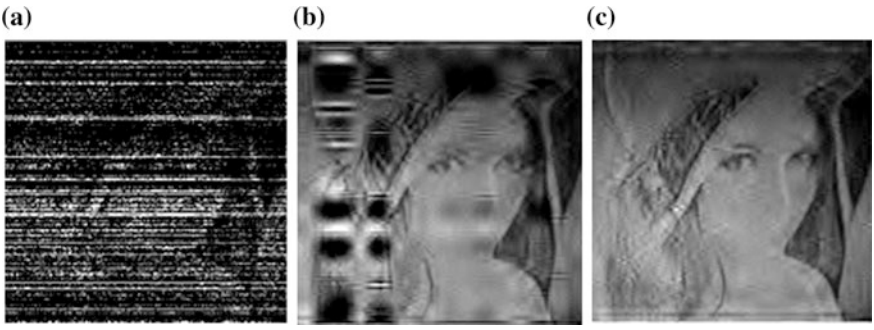

Fig. 7 The reconstruction effect chart of the Lena image. **a** Ratio is 20 %. **b** Ratio is 30 %. **c** Ratio is 40 %

Table 1 The reconstruction time under different measurement ratios of word "天", word "津", and the Lena image

Target image	Measurement ratio (%)	Reconstruction time (s)
The image of word "天"	20	13.75
	30	27.35
	40	43.56
The image of word "津"	20	13.87
	30	28.58
	40	44.54
The Lena image	20	56.56
	30	65.43
	40	75.54

3.1.2 The Experimental Analysis

It can be concluded from Figs. 5, 6, and 7 that under the same measurement ratio, the reconstruction effect of simple Chinese character images is superior to the quietly complex Lena image. By analyzing the data in Table 1, that for the same target image, along with the increase of the measurement ratio, the reconstructed image has a more clear effect, and the reconstruction time is in continual increase. Under the same measurement ratio, the Lena image needs the longest reconstruction time. Therefore, coming to a conclusion that GPSR reconstruction algorithm combining with polynomial measurement matrix based on gram matrix, along with the increase of the complexity of the image, the reconstruction time will increase.

3.2 *Experiment 2: SAMP Algorithm Combining with Hada Code Measurement Matrix Based on Pseudo-random Sequence*

3.2.1 The Experimental Data

SAMP reconstruction algorithm adopted in this experiment was combining with Hada code measurement matrix based on pseudo-random sequence, was divided into three groups. Figure 8 shows the reconstruction effect of word "天" under different measurement ratios, Fig. 9 shows the corresponding reconstruction effect of word "津" under different measurement ratios. Figure 10 shows the reconstruction effect of the Lena image under the different measurements ratios. Table 2 shows the reconstruction time in each group under the different measurement ratios.

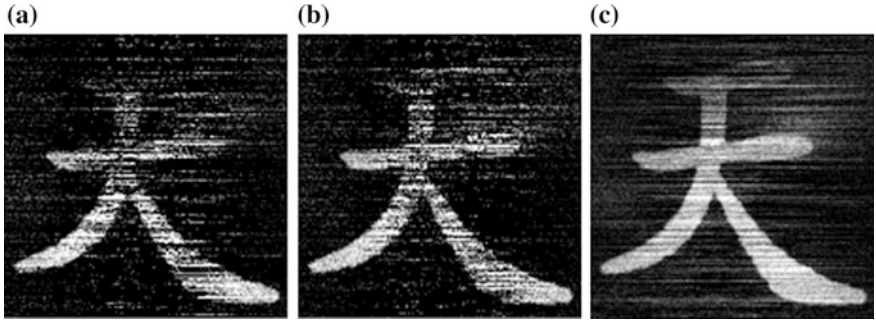

Fig. 8 The reconstruction effect chart of word "天". **a** Ratio is 20 %. **b** Ratio is 30 %. **c** Ratio is 40 %

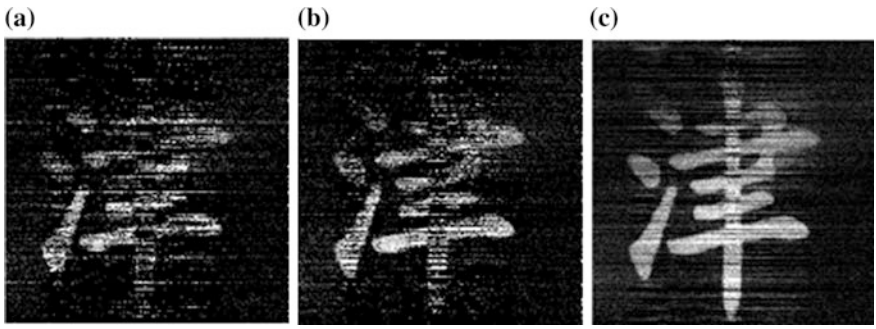

Fig. 9 The reconstruction effect chart of word "津". **a** Ratio is 20 %. **b** Ratio is 30 %. **c** Ratio is 40 %

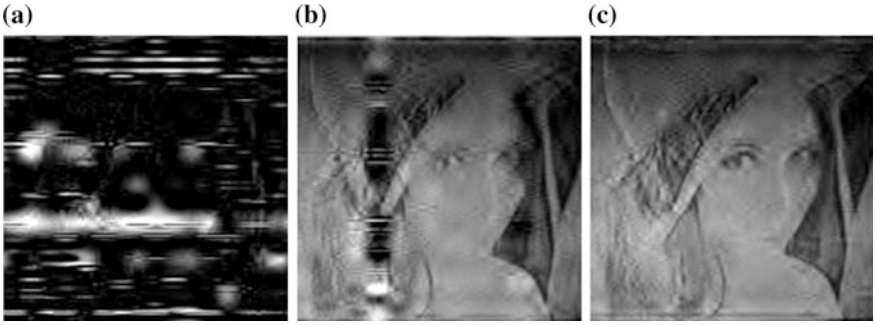

Fig. 10 The reconstruction effect chart of the Lena image. **a** Ratio is 20 %. **b** Ratio is 30 %. **c** Ratio is 40 %

Table 2 The reconstruction time under different measurement ratios of word "天", word "津", and the Lena image

Target Image	Measurement ratio (%)	Reconstruction time (s)
The image of word "天"	20	23.75
	30	22.35
	40	21.56
The image of word "津"	20	22.87
	30	21.58
	40	20.54
The Lena image	20	37.54
	30	36.43
	40	35.54

3.2.2 The Experimental Analysis

Observing from Figs. 8, 9, and 10, it can be concluded that, under the same measurement ratio, the reconstruction effect of simple Chinese character images is superior to the quietly complex Lena image. By analyzing the data in Table 2, for the same target image, along with the increase of the measurement ratio, the reconstructed image has a more clear effect, and the reconstruction time is in continual reduce. Under the same measurement ratio, the Lena image needs the longest reconstruction time. Therefore, it can come to a conclusion that SAMP reconstruction algorithm combining with polynomial measurement matrix based on gram matrix, along with the increase of the complexity of the image, the reconstruction time will increase.

3.3 The Compare and Analysis of the Results of Experiment 1 and Experiment 2

Analyzing the results of the two experiments, comparing Fig. 5 with Fig. 8, Fig. 6 with Fig. 9, and Fig. 7 with Fig. 10, the reconstruction effect of experiment 2 is superior to the experiment 1. Comparing Table 1 with Table 2, only when measurement ratio is 20 %, the reconstruction time of experiment is longer than experimental 1; and when measurement ratio is 30 % or 40 %, the reconstruction time of experiment is less than experimental 1. For the same target images, along with the increase of the measurement ratio, reconstruction time of experimental 1 become longer, reconstruction time of experimental 2 is reduced gradually.

As has been analyzed above, we can conclude that SAMP reconstruction algorithm combining with Hada code measurement matrix based on pseudo-random sequence is superior to GPSR reconstruction algorithm combining with polynomial measurement matrix based on gram matrix.

4 Conclusions

In this paper, two algorithms in image acquisition system based on compressed sensing on the hardware platform is introduced, and the results of the two groups of experimental data show that these two algorithms provide a viable option for the design of the image acquisition system based on the compressed sensing. SAMP reconstruction algorithm combining with Hada code measurement matrix based on pseudo-random sequence has a very important significance in designing the practical-value image acquisition system based on the compressed sensing.

Acknowledge This paper is supported by Natural Science Foundation of China (61271411), and cooperation project of 2014 annual national natural science fund committee with the Edinburgh royal society of British (613111215). It also supported by Tianjin Research Program of Application Foundation and Advanced Technology (15JCZDJC31500), National Natural Science Foundation of China (Grant No. 61501326), and Research on real time topology optimization and efficient broadcasting transmission algorithm in ZigBee networks for smart grid(NSFC:61401310).

References

1. Li Guike, Li Yulong, Feng Peng et al (2009) A novel single-Poly floating-gate UV sensor using standard CMOS process. Proc SPIE 7385:73852B
2. Stern A, Rivenson Y, Javidi B (2008) Single exposure optically compressed imaging and visualization using random aperture coding. J Phys 139:1–10
3. Deng Cai, He Xiaofei, Han Jiawei, TS Huang (2011) Graph regularized non-negative matrix factorization for data representation. IEEE Trans Pattern Anal Mach Intell 33(8):1548–1560

4. Merrett GV, Harris NR, A-l Hashimi BM (2007) Energy managed reporting for wireless sensor network. Sens Actuators 4:1–11
5. Wu L, Weaver C, Austin T (2001) A fast flexible architecture for secure communication. In: Proceedings of the 28th annual international symposium on computer architecture, Göteborg, Sweden
6. Fiskiran AM, Lee RB (2005) On-chip lookup tables for fast symmetric-key encryption. In: Proceedings of IEEE international conference on application-specific systems, architecture processors, Samos, Greece
7. Bigas M, Cabruja E, Forest J et al (2006) Review of CMOS image sensors. Microelectron J 37 (5):433–451
8. Lustig Michael, Donoho David, Pauly John M (2007) Sparse MRI: the application of compressed sensing for rapid MR imaging. Magn Reson Med 58(6):1182–1195
9. Ke Jun, Shankar Premchandra, Neifeld Mark A (2009) Distributed imaging using an array of compressive cameras. Optics Commun 282:185–197
10. Lei Xu, Liang Qilian, Cheng Xiuzhen, Chen Dechang (2013) Compressive sensing in distributed radar sensor networks using pulse compression waveforms. EURASIP J Wirel Commun Netw. doi:10.1186/1687-1499-2013-36